Proceedings of IEDTC07
Proceedings of the 6th ASME International Conference on Multibody Systems, Nonlinear Dynamics and Control
September 4-7, 2007, Las Vegas, Nevada, USA

DETC2007-35666

A DISCUSSION OF LOW ORDER NUMERICAL INTEGRATION FORMULAS FOR RIGID AND FLEXIBLE MULTIBODY DYNAMICS

Naresh Khude
Dept. Mech. Engineering
University of Wisconsin, Madison, WI
Email: khude@wisc.edu

Laurent O. Jay
Dept. Mathematics
University of Iowa, Iowa-City, IA
Email: ljay@math.uiowa.edu

Andrei Schaffer
MSC.Software
Ann Arbor, MI
Email: andrei.schaffer@mscsoftware.com

Dan Negrut*
Dept. Mech. Engineering
University of Wisconsin, Madison, WI
Email: negrut@wisc.edu

ABSTRACT

The premise of this work is that real-life mechanical systems limit the use of high order integration formulas due to the presence in the associated models of friction and contact/impact elements. In such cases producing a numerical solution necessarily relies on low order integration formulas. The resulting algorithms are generally robust and expeditious; their major drawback remains that they typically require small integration stepsizes in order to meet a user prescribed accuracy. This paper looks at three low order numerical integration formulas: Newmark, HHT, and BDF of order two. These formulas are used in two contexts. A first set of three methods is obtained by considering a direct index-3 discretization approach that solves for the equations of motion and imposes the position kinematic constraints. The second batch of three additional methods draws on the HHT and BDF integration formulas and considers in addition to the equations of motion both the position and velocity kinematic constraint equations. The first objective of this paper is to review the theoretical results available in the literature regarding the stability and convergence properties of these low order methods when applied in the context of multibody dynamics simulation. When no theoretical results are available, numerical experiments are carried out to gauge order behavior. The second objective is to perform a set of numerical experiments to compare these six methods in terms of several metrics: (a) efficiency, (b) velocity constraint drift, and (c) energy preservation. A set of simple mechanical systems is used for this purpose: a double pendulum, a slider crank with rigid bodies, and a slider crank with a flexible body represented in the floating frame of reference formulation.

INTRODUCTION

A multitude of phenomena, processes, and applications are described in terms of mixed systems of differential equations combined with linear and nonlinear algebraic equations, most often corresponding to models coming from engineering, physics, and chemistry. Differential equations relate certain quantities to their derivatives with respect to time and/or space variables. Algebraic equations usually model conservation laws and the constraints present in the system. When there are derivatives with respect to only one independent variable (usually time) the equations are called differential-algebraic equations (DAEs). DAEs are basically differential equations defined on submanifolds of $\mathbb{R}^n$. The constrained equations of motion can be expressed in the

*Address all correspondence to this author.

form (see, for instance, [1,2])

$$\begin{aligned} \dot{\mathbf{q}} &= \mathbf{v} \\ \mathbf{M}(\mathbf{q})\dot{\mathbf{v}} &= \mathbf{Q}(t,\mathbf{q},\mathbf{v},\lambda,\mu,\mathbf{u}(t)) - \Phi_{\mathbf{q}}^T(\mathbf{q},t)\lambda - \Gamma_{\mathbf{v}}^T(\mathbf{v},\mathbf{q},t)\mu \\ \mathbf{0} &= \Phi(\mathbf{q},t) \\ \mathbf{0} &= \Gamma(\mathbf{v},\mathbf{q},t) \end{aligned} \tag{1}$$

where $\mathbf{q} \in \mathbb{R}^n$ are generalized coordinates, $\mathbf{v} \in \mathbb{R}^n$ are generalized velocities, $\lambda \in \mathbb{R}^m$ and $\mu \in \mathbb{R}^p$ are Lagrange multipliers, and $\mathbf{u} : \mathbb{R} \to \mathbb{R}^c$ represent time dependent external dynamics; e.g., control variables. The matrix $\mathbf{M}(\mathbf{q})$ is the generalized mass matrix, $\mathbf{Q}(t,\mathbf{q},\mathbf{v},\lambda,\mu,\mathbf{u}(t))$ represents the vector of generalized forces, $\Phi(\mathbf{q},t)$ is the set of m holonomic constraints, i.e., position-level kinematic constraints, and $\Gamma(\mathbf{v},\mathbf{q},t)$ is the set of p nonholonomic constraints, i.e., velocity-level kinematic constraints ([1,3,4]). Differentiating the kinematic constraints with respect to time leads to the additional equations

$$\begin{aligned} \mathbf{0} &= \Phi_{\mathbf{q}}(\mathbf{q},t)\mathbf{v} + \Phi_{\mathbf{t}}(\mathbf{q},t) \\ \mathbf{0} &= \Phi_{\mathbf{q}}(\mathbf{q},t)\dot{\mathbf{v}} + (\Phi_{\mathbf{q}}(\mathbf{q},t)\mathbf{v})_{\mathbf{q}}\mathbf{v} + 2\Phi_{\mathbf{q}t}(\mathbf{q},t)\mathbf{v} + \Phi_{tt}(\mathbf{g},t) \\ \mathbf{0} &= \Gamma_{\mathbf{v}}(\mathbf{v},\mathbf{q},t)\dot{\mathbf{v}} + \Gamma_{\mathbf{q}}(\mathbf{v},\mathbf{q},t)\mathbf{v} + \Gamma_t(\mathbf{v},\mathbf{q},t). \end{aligned} \tag{2}$$

Equations (1) and (2) form an over-determined system of DAEs, having strictly more equations than variables. The ability to solve such systems is relevant for several classes of applications such as multibody dynamics and molecular dynamics.

When finding the solution of Eqs. (1) and (2), most numerical solvers currently used in industry share some or all of the following major drawbacks: numerical drift that occurs when the solution does not stay on the manifold of constraints at the position and/or velocity levels and as such might become nonphysical; inability to deal efficiently with stiffness; loss of underlying properties of the exact flow and trajectories; no preservation of invariants such as energy; introduction of undesired numerical damping; and the reduction of convergence order when solving stiff problems that arise often in applications. Whereas techniques for the numerical solution of ordinary differential equations (ODEs) go back more than three centuries and are well established, the numerical solution of DAEs has a comparatively short history ([5–7]). The first class of numerical techniques applied to DAEs was published in [8] for the solution of ODEs. Since then DAEs have widely penetrated the numerical analysis, engineering, and scientific computing communities and are increasingly encountered in practical applications. Still, numerically solving DAEs poses fundamental difficulties not encountered when solving ODEs. Therefore, specialized numerical techniques have been developed, typically belonging to one of two classes: state-space methods or direct methods.

State-space methods first reduce the DAEs to a smaller dimension ODE problem, thus benefiting from the extensive body of knowledge associated with ODE solvers. Specifically, the DAEs induce differential equations on the constraint manifold [9], which can be reduced on a subspace of the n-dimensional Euclidean space. The resulting state-space ODEs (SSODEs) are integrated using classical numerical integration formulas. The one-to-one local mapping from the manifold to the subspace of independent coordinates is then used to determine the point on the manifold corresponding to the solution of the SSODEs. This framework formalizes the theory of numerical solution of DAEs using the language of differential manifolds [10]. Practical approaches in this class of methods are presented in [9, 11–13]. The main factor that differentiates these approaches is the choice of manifold parameterization. State-space methods have been subject to criticism in two aspects. First, the choice of parameterization generally is not global. Second, poor choices of the projection space result in SSODEs that are numerically demanding, mainly at the expense of overall efficiency and robustness of the algorithm [14]. Although the theoretical framework for these methods was outlined several years ago [9, 15], it was only recently that implicit numerical integration methods for DAEs have been proposed in the context of SSODEs for multibody dynamics analysis [16, 17]. The major intrinsic drawback associated with state-space methods remains the expensive DAE to ODE reduction process that is further exacerbated in the context of implicit integration, which is the norm in industry applications.

Alternatively, direct methods discretize the constrained equations of motion (Eq. (1)), possibly after reducing the index of the DAEs by considering some or all of the kinematic constraint equations in Eq. (2). Original contributions in this direction are found in [5, 18–25]. When dealing with systems that include flexible substructures and bodies, numerical methods have been sought that are capable of introducing controllable numerical dissipation to damp out spurious high frequencies, which are an artifact of the spatial discretization, without affecting the low frequencies of the system and the accuracy of the method [26, 27]. Several methods have been proposed for structural dynamic simulation, such as the HHT method (also called α-method) [28] and the generalized α-method [29]. These are order two methods proposed in conjunction with ODE problems associated with structural dynamics. For constrained multibody systems only a few α-type algorithms capable of addressing the nonlinear algebraic component associated with the DAE problem have been reported in the literature [30, 31]. Recent theoretical and implementation aspects related to an HHT-based numerical integrator for the simulation of large mechanical systems with flexible bodies and contact/impact have been discussed in [32]. One of the salient attributes of their algorithm is the good condition number of the Jacobian associated with the implicit numerical integrator. Building on a scaling idea introduced in conjunction with BDF methods in [5] and recently discussed in [33], the condition number remains bounded when $h \to \infty$. Furthermore, the proposed method effectively "filters out" errors in cer-

tain partial derivatives that might be introduced, for instance, by approximations of external loading (tires, aerodynamic forces, etc.), thanks to the scaling by h^2. The attractive attributes of the method proposed in [32] are overshadowed by two drawbacks. First, there is no global proof of convergence associated with the method, although extensive numerical experiments indicate second order convergence. Second, the method imposes only the position-level constraint equations, which leads to a violation of the velocity-level constraint equations.

INTEGRATION FORMULAS

The first numerical integration method considered here draws on the Newmark formulas [34]. It requires the selection of two parameters $\gamma \geq 1/2$, $\beta \geq (\gamma+1/2)^2/4$ based on which, given the acceleration $\ddot{\mathbf{q}}_{n+1}$ at the new time step t_{n+1}, the new position and velocity are obtained as

$$\begin{aligned} \mathbf{q}_{n+1} &= \mathbf{q}_n + h\dot{\mathbf{q}}_n + \tfrac{h^2}{2}\left[(1-2\beta)\ddot{\mathbf{q}}_n + 2\beta\ddot{\mathbf{q}}_{n+1}\right] \\ \dot{\mathbf{q}}_{n+1} &= \dot{\mathbf{q}}_n + h\left[(1-\gamma)\ddot{\mathbf{q}}_n + \gamma\ddot{\mathbf{q}}_{n+1}\right] \end{aligned} \tag{3}$$

In the context of a multibody dynamics, using an integration step size h , the discretization scheme operates on the constrained equations of motion and position kinematic constraint equations to lead to the nonlinear system:

$$(\mathbf{M}\ddot{\mathbf{q}})_{n+1} + (\Phi_q^T\lambda)_{n+1} = \mathbf{Q}_{n+1} \tag{4}$$

$$\Phi(\mathbf{q}_{n+1}, t_{n+1}) = \mathbf{0} \tag{5}$$

The method, called hereafter NEWMARK, is first order unless $\gamma = 1/2$ and $\beta = 1/4$. This choice leads to the trapezoidal method, which is known in the literature to have stability problems when used on index-3 DAEs.

Referred to as HHT-I3, the second method considered in this study draws on the HHT method [28], which has been widely used in the structural dynamics community and later used in the context of multibody dynamics analysis [30]. HHT-I3 represents a slight variation of the NEWMARK method in that it still uses the same discretization formulas of Eq. (3) but alters the equation of motion:

$$(\mathbf{M}\ddot{\mathbf{q}})_{n+1} + (1+\alpha)(\Phi_q^T\lambda - \mathbf{Q})_{n+1} - \alpha(\Phi_q^T\lambda - \mathbf{Q})_n = \mathbf{0} \tag{6}$$

The third integration method considered in this study is essentially the BDF method of order two proposed in [8]. This method is cast into a form similar to the Newmark formula:

$$\begin{aligned} \mathbf{q}_{n+1} &= \tfrac{4}{3}\mathbf{q}_n - \tfrac{1}{3}\mathbf{q}_{n-1} + h\left(\tfrac{8}{9}\dot{\mathbf{q}}_n - \tfrac{2}{9}\dot{\mathbf{q}}_{n-1}\right) + \tfrac{4}{9}h^2\ddot{\mathbf{q}}_{n+1} \\ \dot{\mathbf{q}}_{n+1} &= \tfrac{4}{3}\dot{\mathbf{q}}_n - \tfrac{1}{3}\dot{\mathbf{q}}_{n-1} + \tfrac{2}{3}h\ddot{\mathbf{q}}_{n+1} \end{aligned} \tag{7}$$

These formulas used in conjunction with Eq. (4) and (5) lead to a second order method referred to in the sequel as NSTIFF.

The next three numerical integration methods investigated herein take into account the velocity kinematic constraint equations to prevent drift in velocity constraints and improve the overall quality of the solution. One of these methods introduces a correction into the Newmark formulas based on the constraint accelerations and was shown to have global convergence order two [35]. Given an initial configuration $(\mathbf{q}_0, \dot{\mathbf{q}}_0, \ddot{\mathbf{q}}_0)$, and defining $\mathbf{f}(t,\mathbf{q},\dot{\mathbf{q}}) := \mathbf{M}^{-1}(\mathbf{q})\,\mathbf{Q}(t,\mathbf{q},\dot{\mathbf{q}})$ and $\mathbf{r}(\mathbf{q},\lambda) := -\mathbf{M}^{-1}(\mathbf{q})\Phi_q^T\lambda$,

$$\begin{aligned} \mathbf{q}_1 &= \mathbf{q}_0 + h\dot{\mathbf{q}}_0 + \tfrac{h^2}{2}((1-2\beta)\ddot{\mathbf{q}}_0 + 2\beta\ddot{\mathbf{q}}_1) \\ &\quad + \tfrac{h^2}{2}((1-b)\mathbf{R}_0 + b\mathbf{R}_1) \\ \dot{\mathbf{q}}_1 &= \dot{\mathbf{q}}_0 + h((1-\gamma)\ddot{\mathbf{q}}_0 + \gamma\ddot{\mathbf{q}}_1) + \tfrac{h}{2}(\mathbf{R}_0 + \mathbf{R}_1) \\ \mathbf{0} &= \Phi(\mathbf{q}_{n+1}, t_{n+1}) \\ \mathbf{0} &= \Phi_{\mathbf{q}}(\mathbf{q}_1, t_1)\dot{\mathbf{q}}_1 + \Phi_t(\mathbf{q}_1, t_1) \\ \ddot{\mathbf{q}}_1 &= (1+\alpha)\mathbf{f}(t_1, \mathbf{q}_1, \dot{\mathbf{q}}_1) - \alpha\mathbf{f}(t_0, \mathbf{q}_0, \dot{\mathbf{q}}_0) \end{aligned} \tag{8}$$

where $b \neq 1/2$ is a free coefficient, $\mathbf{R}_0 := \mathbf{r}(t_0, \mathbf{q}_0, \psi_0)$, $\mathbf{R}_1 := \mathbf{r}(t_1, \mathbf{q}_1, \psi_1)$, and ψ_0 , ψ_1 are determined at each time step by imposing that the position and velocity kinematic constraint equations hold at time t_1. This method is referred as HHT-ADD and discussed at length in [35, 36].

The fifth integration method investigated, HHT-SI2, is a variation on the above formula [37]. The following discretization formulas, in conjunction with the position and velocity kinematic constraint equations, leads to a second order method:

$$\mathbf{q}_1 = \mathbf{q}_0 + h\dot{\mathbf{q}}_0 + \frac{h^2}{2}\left((1-2\beta)\,\ddot{\mathbf{q}}_\alpha + 2\beta\tilde{\mathbf{a}}_{1+\alpha}\right) \tag{9}$$

$$\dot{\mathbf{q}}_1 = \dot{\mathbf{q}}_0 + h\left((1-\gamma)\,\ddot{\mathbf{q}}_\alpha + \gamma\ddot{\mathbf{q}}_{1+\alpha}\right) \tag{10}$$

$$\mathbf{M}_{1+\alpha}\tilde{\mathbf{a}}_{1+\alpha} = (1+\alpha)\,\mathbf{f}\left(t_1, \mathbf{q}_1, \dot{\mathbf{q}}_1, \tilde{\lambda}_1\right) - \alpha\,(t_0, \mathbf{q}_0, \dot{\mathbf{q}}_0, \lambda_0) \tag{11}$$

$$\mathbf{M}_{1+\alpha}\ddot{\mathbf{q}}_{1+\alpha} = (1+\alpha)\,\mathbf{f}(t_1, \mathbf{q}_1, \dot{\mathbf{q}}_1, \lambda_1) - \alpha\,(t_0, \mathbf{q}_0, \dot{\mathbf{q}}_0, \lambda_0) \tag{12}$$

where $\mathbf{M}_{1+\alpha} := \mathbf{M}\,(t_{1+\alpha}, \mathbf{q}_0 + h(1+\alpha)\dot{\mathbf{q}}_0)$ and $\tilde{\mathbf{a}}_{1+\alpha}$, $\tilde{\lambda}_1$ are auxiliary variables which are local to the current time step.

Finally, the sixth and last integration method investigated in this work is the so called stabilized index 2 formulation [19] that uses the discretization formulas of Eq. (7) and solves the following system of nonlinear equations to recover the state of the mechanical system at time-step t_{n+1}:

$$\mathbf{v}_{n+1} = \dot{\mathbf{q}}_{n+1} + \left(\Phi_{\mathbf{q}}^T\mu\right)_{n+1} \tag{13}$$

$$(\mathbf{M}(\mathbf{q})\dot{\mathbf{v}})_{n+1} = \mathbf{Q}(t_{n+1}, \mathbf{q}_{n+1}, \mathbf{v}_{n+1}) - \Phi_{\mathbf{q}}^T\lambda \tag{14}$$

$$\Phi(\mathbf{q}_{n+1}, t_{n+1}) = \mathbf{0} \tag{15}$$

$$\Phi_{\mathbf{q}}(\mathbf{q}_{n+1}, t_{n+1})\,\mathbf{v}_{n+1} + \Phi_t(\mathbf{q}_{n+1}, t_{n+1}) = \mathbf{0} \tag{16}$$

Like HHT-SI2, this integration method relies on the discretization of the kinematic velocity constraint equations and the use of an auxiliary variable to prevent velocity drift. This method is referred to as NSTIFF-SI2 and is a second order integration method [19].

Among these integration methods, NSTIFF, HHT-ADD, HHT-SI2, and NSTIFF-SI2 have global convergence proofs for the class of DAEs associated with multibody dynamics [35–39]. However, theoretical global convergence results for NEWMARK and HHT-I3 are, to the best of our knowledge, not available yet. Nonetheless, numerical experiments carried out suggest that even in case of index 3 DAEs, these methods display convergence orders that have been proved for the ODE case (one and two, respectively). A formal proof for this is yet to be produced.

NUMERICAL EXPERIMENTS

The set of six numerical algorithms discussed in the previous section were implemented and used in conjunction with a set of three models. Several experiments were run to evaluate the algorithms' performance and compare them in relation to the order of global convergence, energy preservation, constraint satisfaction and efficiency.

Models Considered

The models considered for testing and comparison of algorithm performance are the double pendulum, slider crank, and slider crank with flexible link using floating frame of reference formulation [2]. The model parameters and the initial conditions used are summarized below.

a. Double Pendulum
Figure 1 shows the schematic of a double pendulum. Torsional spring and dampers are included in the model at the pin joints. The parameter values used in this model are m_1 = 3 kg, L_1 = 1 m, k_1 = 400 N/m, c_1 = 15 Ns/m, m_2 = 0.3 kg, L_2 = 1.5 m, k_2 = 300000 N/m and c_2 = 5000 Ns/m. The initial conditions were $\theta_1(0) = 0$, $\theta_2(0) = \frac{23\pi}{12}$, $\dot{\theta}_1(0) = 0$ and $\dot{\theta}_2(0) = 10$. Units throughout the paper are SI unless indicated otherwise.

b. Slider Crank
The schematic of a slider crank model including a spring-damper element is shown in Figure 2. The parameters associated with the model are m_1 = 3 kg, L_1 = 0.3 m, m_2 = 0.9 kg, L_2 = 0.6 m, k = 100 N/m and c = 5 Ns/m.
The initial conditions used for simulation of motion were $\theta_1(0) = 3\pi/2$, $\dot{\theta}_1(0) = 0$ rad/s.

c. Flexible Slider Crank
This model is similar to the rigid slider-crank shown in Figure 2, except that the spring and damper are not included and the connecting rod is flexible. The parameter values used in this model are m_1 = 3 kg, L_1 = 0.3 m, m_2 = 0.9 kg and L_2 = 0.6 m, cross-section area A = 5.74E-6 m^2, moment of inertia I = 2.765E-8 m^4 and Young's modulus E = 200 GPa. The initial conditions are $\theta_1(0) = 3\pi/2$, $\dot{\theta}_1(0) = 1$ rad/s. The equations of motion are formulated using the floating frame of reference formulation [2].

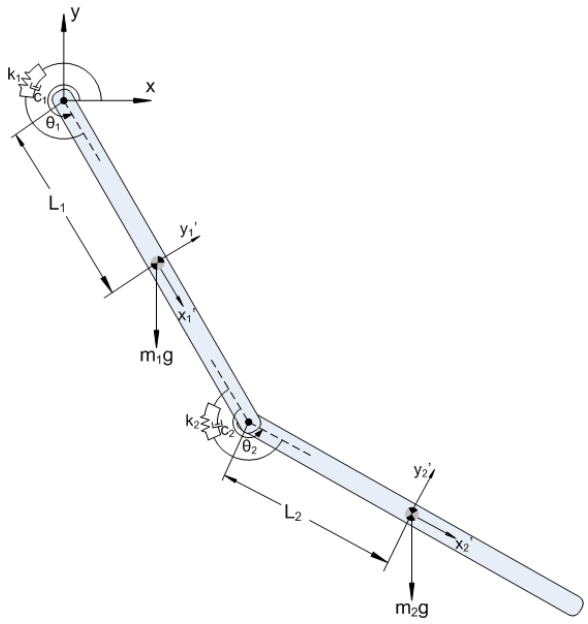

Figure 1. Double Pendulum

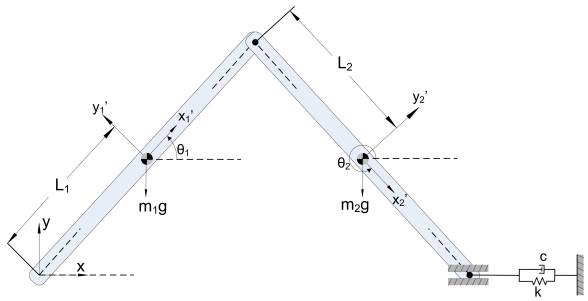

Figure 2. Slider Crank

Order analysis

To investigate the convergence order of each numerical method, a reference solution for each model is determined by first deriving a set of second order ODEs that govern the time evolution of the system. This ODE problem is subsequently solved using a fourth order Runge-Kutta method (see, for instance, [7]) with a step size of $h = 10^{-6}$ s. The exception was the flexible slider crank model, for which the reference solution was obtained with HHT-ADD with a step size of $h = 10^{-6}$. Each

model is simulated for 2 seconds and the results are compared to the reference solution based at the final time. Results show that NSTIFF, HHT-SI2, HHT-ADD, NSTIFF-SI2 exhibit order 2 convergence, in line with theoretical results established in conjunction with these algorithms. Furthermore, HHT-I3 (for nonzero values of α) and NEWMARK show global convergence of order 2 and 1, respectively, for all the models. To the best of our knowledge there are no analytical results to explain the numerical convergence results obtained for HHT-I3 and NEWMARK. Several convergence plots for each numerical method using considered models are shown in Figs. 3 through 14. Two plots is provided for each convergence analysis: the first one shows the absolute value of the error and it is instrumental in assessing the size of the error when different integrators use the same constant integration step-size to advance the simulation. In this context, the numerical simulations carried out suggest that the most accurate algorithm is HHT-ADD. The second figure for each experiment shows a plot of the slope of the convergence curve. As anticipated, the slope is one for NEWMARK and two for the remaining algorithms.

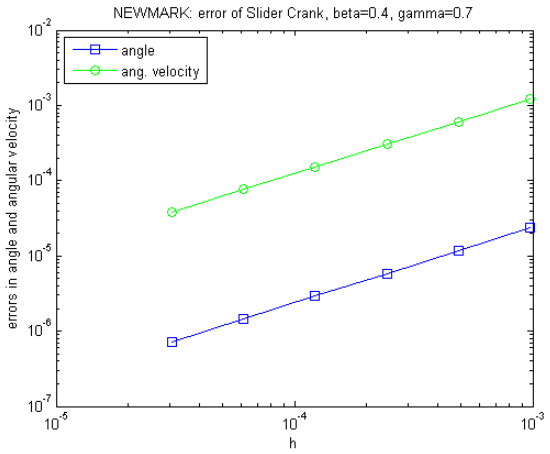

Figure 3. NEWMARK Order Analysis: Slider Crank

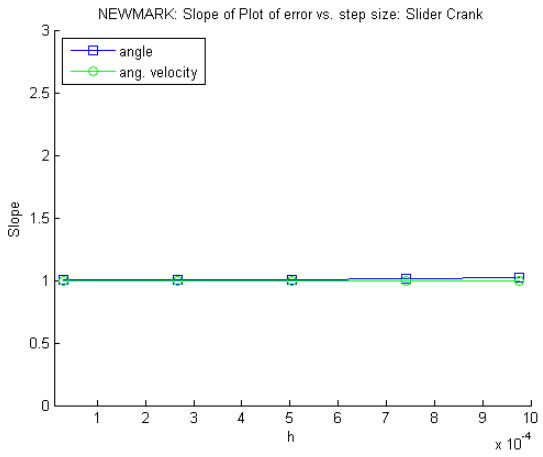

Figure 4. NEWMARK Convergence Order: Slider Crank

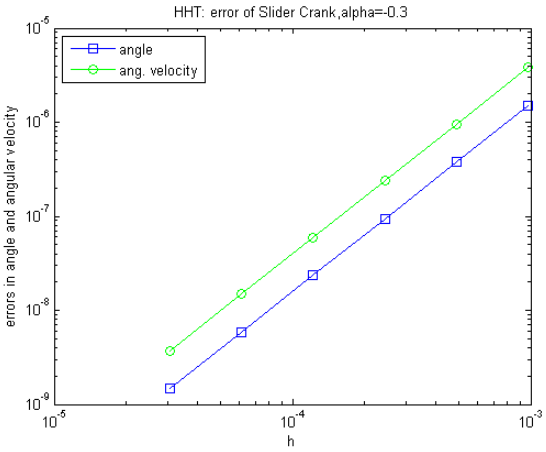

Figure 5. HHTI3 Order Analysis: Slider Crank

Energy preservation

The HHT method came as an improvement over Newmark formulas because it preserved the A-stability and its attractive numerical damping properties while achieving second-order accuracy. In this method, high-frequency oscillations that are of no interest as well as parasitic high-frequency oscillations that are a byproduct of the finite element discretization are damped out through the parameter α. The choice of α is based on the desired level of damping for a particular model. The more negative the value of α, the more damping is induced in the numerical solution. Note that the choice $\alpha = 0$ leads to the trapezoidal method with no numerical damping. The effect of this damping can be seen from energy preservation plots shown in Figs. 15 and 16. These energy plots are for the slider-crank model from which the translational damper was removed. The system is conservative, and for the particular reference system employed, the total energy should be constant and equal to zero.

As anticipated, for $\alpha = -0.3$ the numerical damping-induced dissipation is more pronounced than the $\alpha = -0.05$ case. Even more relevant is an investigation of how the numerical energy dissipation changes with the step-size. Results in Figure 16 indicate a highly oscillatory pattern. To capture the degree to which a numerical scheme dissipates energy, an average energy

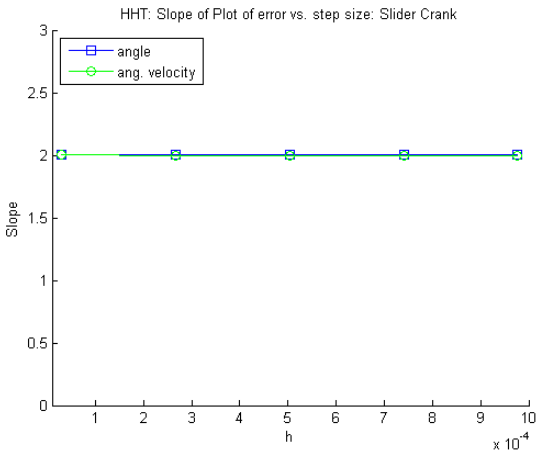

Figure 6. HHTI3 Convergence Order: Slider Crank

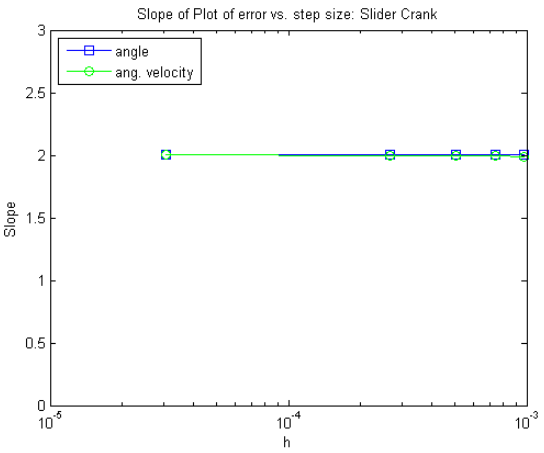

Figure 8. NSTIFF Convergence Order: Slider Crank

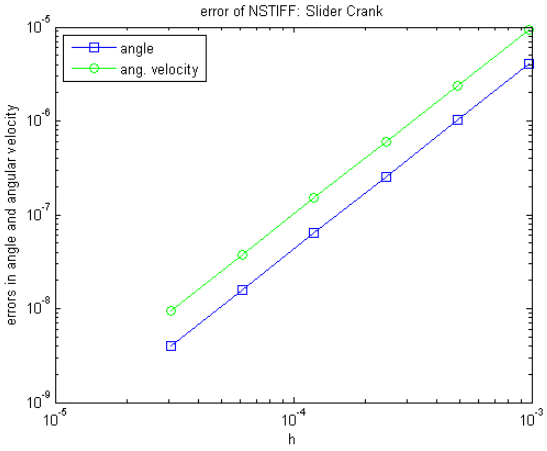

Figure 7. NSTIFF Order Analysis: Slider Crank

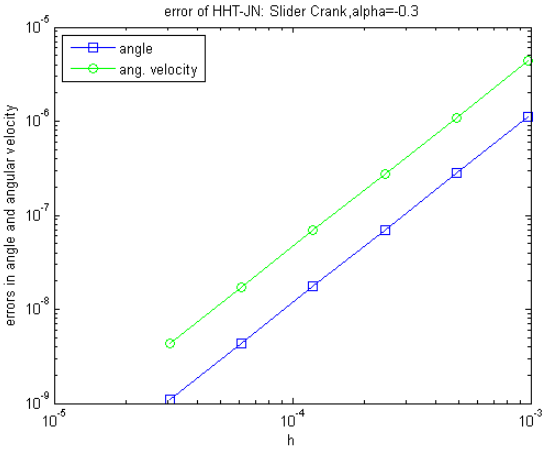

Figure 9. HHT-ADD Order Analysis: Slider Crank

dissipation over an interval $[0,T]$ is computed as

$$\varepsilon(T) = \frac{1}{T}\int_0^T |E_{tot}(t)|\,dt \tag{17}$$

If no numerical dissipation was present in the system then $\varepsilon(T) = 0$, $\forall T > 0$. On a log-log scale, Fig. 17 shows this quantity for the rigid slider crank model with no physical damping, while Fig. 19 displays the same quantity for the flexible slider crank. Surprisingly, this average total energy error converges to zero like $O(h^q)$, where q is the order of the method. In other words, for NEWMARK it converges to zero like $O(h)$, while for all the other methods the average energy error converges like $O(h^2)$.

It remains for this observation vis-à-vis the behavior of $\varepsilon(T)$ to be formally proved. This would be an interesting result in itself, since $\varepsilon(T)$ is a global error that captures the energy drift over the entire simulation. Such a result could be relevant, for instance, in the context of Molecular Dynamics (MD) simulation, since one of the reasons for which entire classes of integrators are disqualified in MD simulation is that they do not preserve energy. However, with values in the femtosecond range, the step-size for MD simulations might be so small that HHT, Newmark, and BDF type methods might in fact be viable candidates in the MD simulation arena. This question is currently under investigation [40].

Kinematic constraint drift

The rationale behind stabilizing the numerical solution of the index 3 DAE of multibody dynamics using the velocity kine-

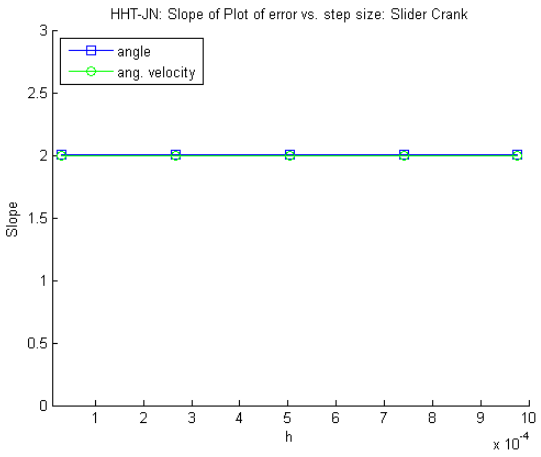

Figure 10. HHT-ADD Convergence Order: Slider Crank

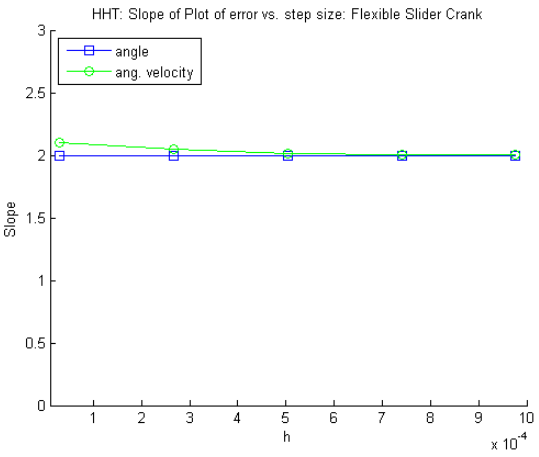

Figure 12. HHT-I3 Convergence Order: Flexible Slider Crank

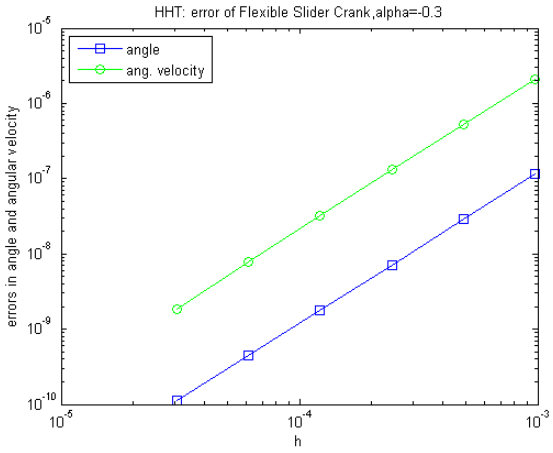

Figure 11. HHT-I3 Order Analysis: Flexible Slider Crank

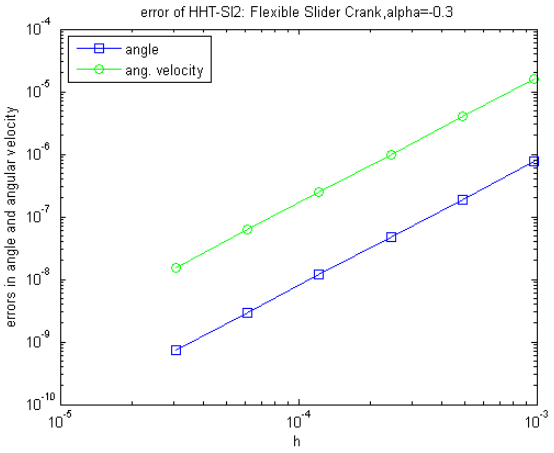

Figure 13. HHT-SI2 Order Analysis: Flexible Slider Crank

matic constraint equations is to prevent drift in satisfying this set of algebraic constraints. Three of the six methods analyzed in this study, namely HHT-ADD, HHT-SI2, and NSTIFF-SI2, enforce these equations. As such, no velocity constraint drift is expected in the numerical solution. This is confirmed by the plots in Figs. 21 through 23. These figures display a plot of the velocity constraint violation in the X direction against the velocity constraint violation in the Y direction for the rigid slider-crank mechanism for the pin joint between the crank and ground. Data was plotted at each time step and, as anticipated, confirms that the velocity kinematic constraint equations are satisfied within machine precision.

Figures 26 through 24 show the same information for the rigid slider crank with no damping; the plots report data obtained during a 10 second long simulation, with a step-size $h = 2^{-10}$s. The most remarkable thing is that NEWMARK, HHT-I3, and NSTIFF display the same error behavior. Moreover, as the step-size decreases, the box that bounds the plot shrinks but the shape of the curves remains the same for all three integration methods. The cause for this behavior remains to be investigated but these results suggest that this limit cycle behavior is a characteristic of the method; i.e., neglecting velocity kinematic constraint equations, rather than of the direct index-3 algorithm used for the numerical solution. For now, it should be pointed out that numerical experiments indicate that the error in satisfying these constraints converges like $O(h^q)$, where q is the order of the method. A more formal investigation of these observations remains to be done in the future. Note that similar plots are obtained when the constraint violation is plotted for the flexible slider crank. For completeness, only the most extreme cases, the results for HHT-ADD

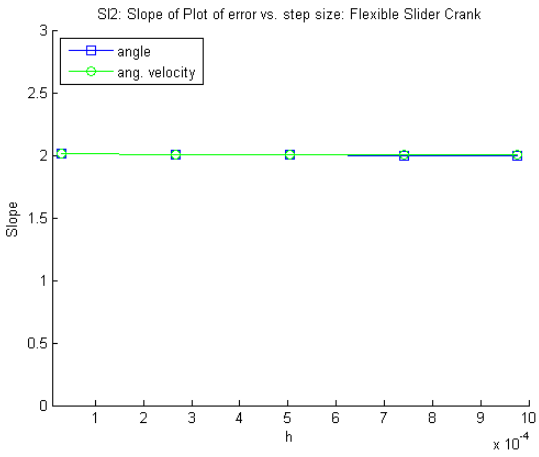

Figure 14. HHT-SI2 Convergence Order: Flexible Slider Crank

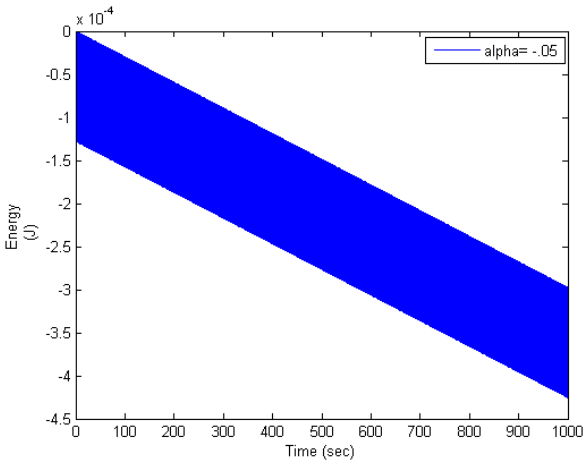

Figure 16. Energy Dissipation at α = - 0.05

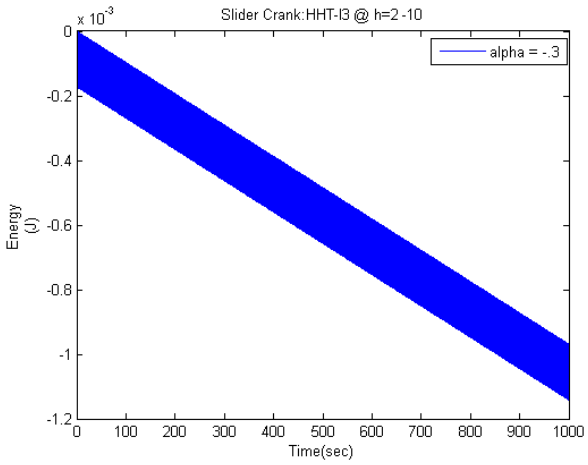

Figure 15. Energy Dissipation at α = - 0.3

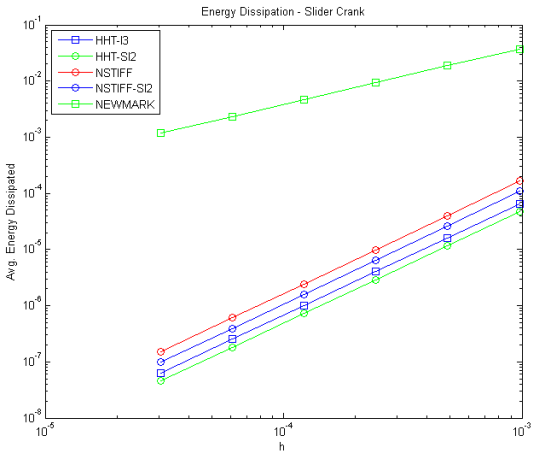

Figure 17. Energy Dissipation Characteristics - Slider Crank

and NEWMARK are reported in Figs. 27 and 28.

Efficiency comparison

The six methods investigated in this work were used to run a 2 second-long simulation of the slider crank model with a constant step-size $h = 2^{-10}$ s. The timing results are reported in Fig. 29, which compares CPU times normalized to the time it takes the HHT-I3 method to finish the simulation. The figure suggests that having the kinematic velocity constraint equations enforced usually leads to an approximately 30% simulation slowdown. As expected, the HHT_ADD is very costly for the flexible body model given that the mass matrix ceases to be constant. This might not be a problem for some more recent formulations [41] where the mass matrix remains constant but it is responsible for the slowdown associated with the floating frame of reference formulation employed for the flexible slider-crank model.

CONCLUSIONS

This paper investigates several low-order numerical integration formulas for determining the time evolution of constrained multibody systems. The motivation for this effort is twofold. First, the vast majority of large real-life models contain discontinuities, friction, and contacts that effectively make low-order integration formulas the only viable, robust candidates capable of handling these classes of problems. Secondly, although less relevant, compared to higher-order implicit formulas, the numer-

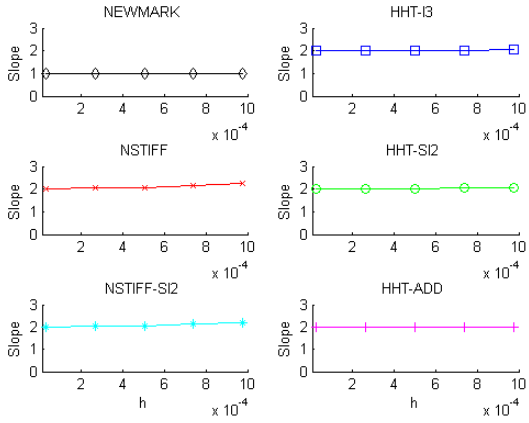

Figure 18. Slope - Energy Dissipation

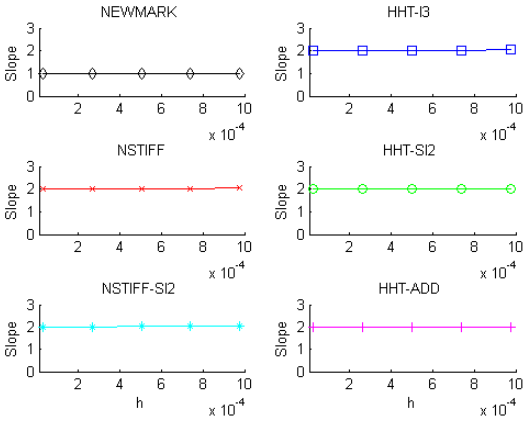

Figure 20. Slope - Energy Dissipation Flexible Slider Crank

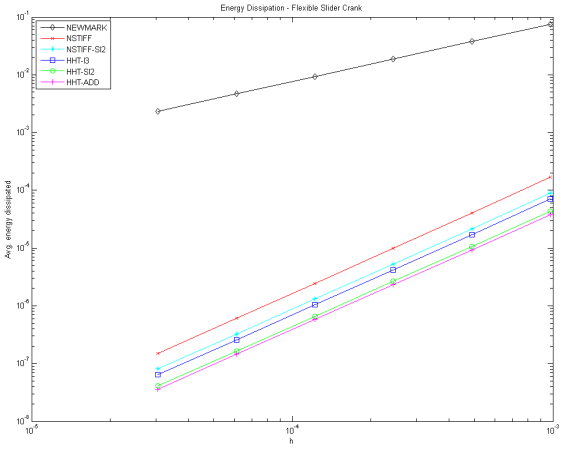

Figure 19. Energy Dissipation - Flexible Slider Crank

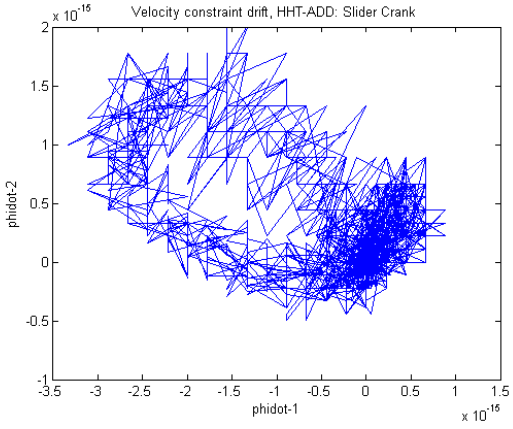

Figure 21. Velocity Constraint Drift - HHT-ADD

ical methods investigated herein are straightforward to implement and some of them are already commonly used in practice. Based on the order convergence and timing results presented, for problems where accurately satisfying the velocity kinematic constraint equations is not a priority, HHT-I3 is a good choice. It is a second order method that has the ability to change the amount of numerical damping that enters the solution process. The major drawback associated with this method is that there is yet no formal proof of the global convergence of the method for value of $\alpha < 0$. While HHT-I3 has been implemented and tested on a large number of complex models and all these results have indicated good robustness and convergence behavior, if one wants to stand on solid theoretical ground then the NSTIFF method is the next best alternative. Global convergence results are available for this second order method and, moreover, our experience indicates that NSTIFF is actually more efficient than HHT-I3. However, the method is plagued by a somewhat more intense numerical damping that cannot be controlled like in HHT-I3. For a slower, but numerically sound approach, one can select the second order HHT-SI2 or NSTIFF-SI2 methods. They are comparable in terms of efficiency, HHT-SI2 having an edge due to its ability to adjust the value of numerical damping introduced into the problem. Preliminary results presented in the paper indicate that satisfying both the position and velocity kinematic constraint equations come at a price of about a 30% increase in simulation time.

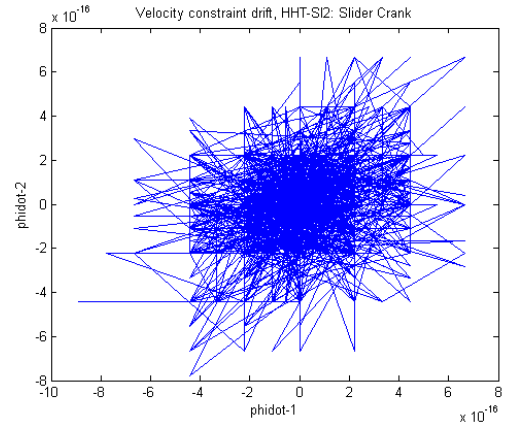

Figure 22. Velocity Constraint Drift - HHT-SI2

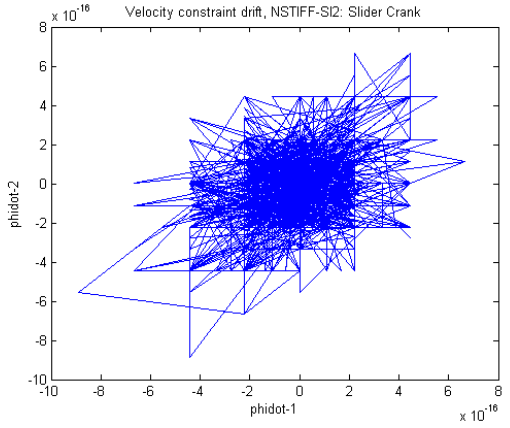

Figure 23. Velocity Constraint Drift - NSTIFF-SI2

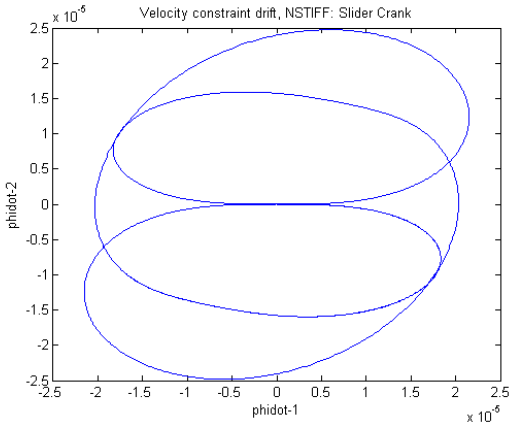

Figure 24. Velocity Constraint Drift - NSTIFF

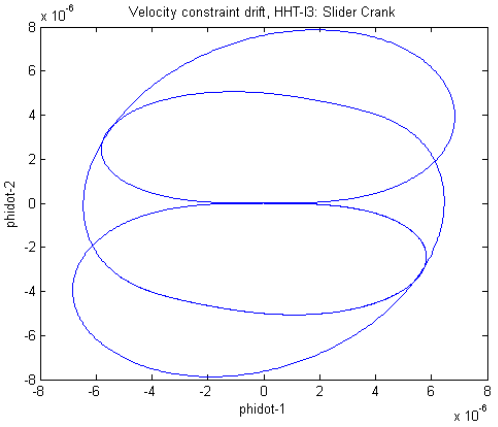

Figure 25. Velocity Constraint Drift - HHT-I3

ACKNOWLEGMENTS

Financial support was provided in part by a gift made by MSC.Software, which is gratefully acknowledged. The authors would like to thank Radu Serban and Nick Schafer for reading the manuscript and providing suggestions for improvement, to Toby Heyn for running the convergence order simulations for the BDF integrators, and Makarand Datar for helping with the typesetting of the document.

REFERENCES

[1] Haug, E. J., 1989. *Computer-Aided Kinematics and Dynamics of Mechanical Systems Volume-I*. Prentice-Hall, Englewood Cliffs, New Jersey.

[2] Shabana, A. A., 2005. *Dynamics of Multibody Systems*, third ed. Cambridge University Press.

[3] Abraham, R., and Marsden, J. E., 1985. *Foundations of Mechanics*. Addison-Wesley., Reading, MA.

[4] Arnold, V., 1989. *Mathematical Methods of Classical Mechanics*. Springer, New York, NY.

[5] Brenan, K. E., Campbell, S. L., and Petzold, L. R., 1989. *Numerical Solution of Initial-Value Problems in Differential-Algebraic Equations*. North-Holland, New York.

[6] Lubich, C., and Hairer, E., 1989. "Automatic integration of the Euler-Lagrange equations with constraints". *J. Comp. Appl. Math.,* **12**, pp. 77–90.

[7] Hairer, E., and Wanner, G., 1991. *Solving Ordinary Differential Equations*, Vol. II of *Computational Mathematics*. Springer-Verlag.

[8] Gear, C. W., 1971. *Numerical Initial Value Problems of Ordinary Differential Equations*. Prentice-Hall, Englewood Cliffs, NJ.

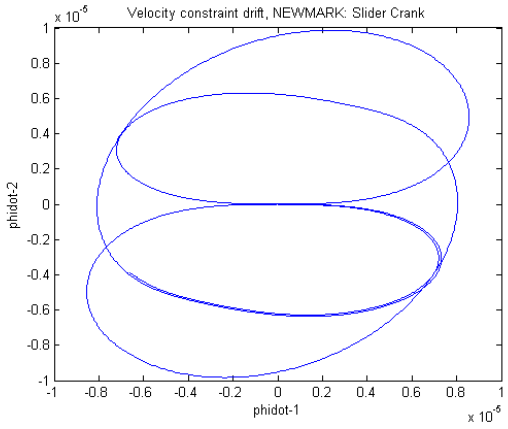

Figure 26. Velocity Constraint Drift - NEWMARK

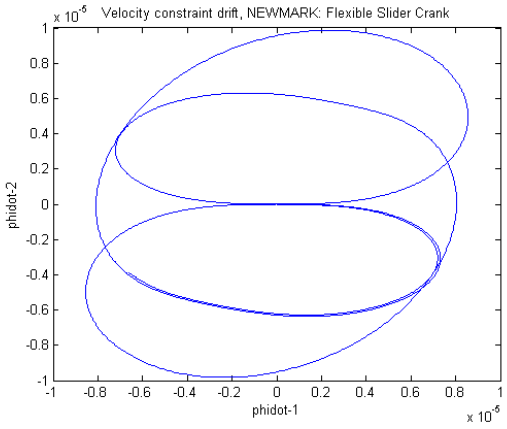

Figure 28. Velocity Constraint Drift - NEWMARK (Flex Slider Crank)

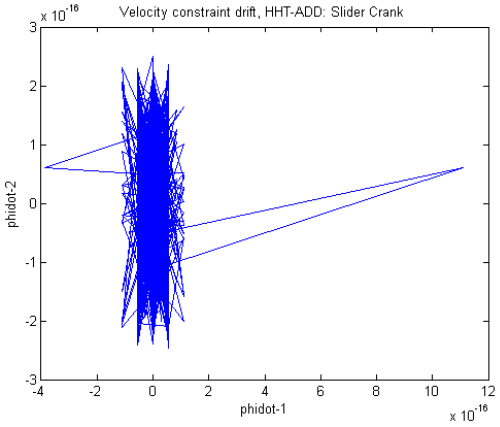

Figure 27. Velocity Constraint Drift - HHT-ADD (Flex Slider Crank)

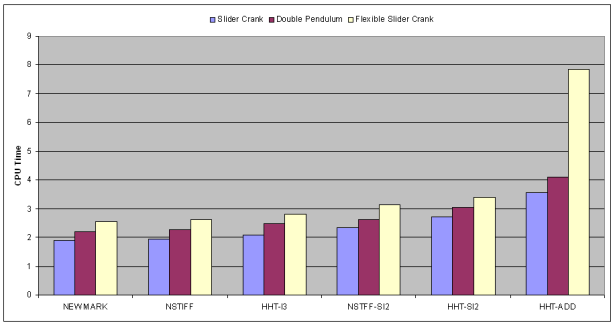

Figure 29. Efficiency comparison (normalized to time of HHT-I3)

[9] W.C.Rheinboldt, and Potra, F., 1991. "On the numerical solution of euler-lagrange equations". *Mechanics of structures and machines*(19(1)), pp. 1–18.

[10] W.C.Rheinboldt, 1984. "Differential-algebraic systems as differential equations on manifolds". *Mathematics of Computation*(Vol. 43), pp. 473–482.

[11] Wehage, R. A., and Haug, E. J., 1982. "Generalized coordinate partitioning for dimension reduction in analysis of constrained dynamic systems". *J. Mech. Design,* **104**, pp. 247–255.

[12] Liang, C. D., and Lance, G. M., 1987. "A differentiable null-space method for constrained dynamic analysis". *ASME Journal of Mechanism, Transmission, and Automation in Design,* **109**, pp. 405–410.

[13] Yen, J., 1993. "Constrained equations of motion in multibody dynamics as odes on manifolds". *SIAM Journal on Numerical Analysis,* **30(2)**, pp. 553–568.

[14] Alishenas, T., 1992. Zur numerischen behandlungen, stabilisierung durch projection und modellierung mechanischer systeme mit nebenbedingungen und invarianten,. PhD Thesis NASA Technical Memorandum 4760, Royal Institute of Technology, Stockholm.

[15] Mani, N., Haug, E., and Atkinson, K., 1985. "Singular value decomposition for analysis of mechanical system dynamics". *ASME Journal of Mechanisms, Transmissions, and Automation in Design,* **107**, pp. 82–87.

[16] Haug, E. J., Negrut, D., and Iancu, M., 1997. "A state-space based implicit integration algorithm for differential-algebraic equations of multibody dynamics". *Mechanics of Structures and Machines,* **25**(3), pp. 311–334.

[17] Negrut, D., Haug, E. J., and German, H. C., 2003. "An implicit Runge-Kutta method for integration of Differential-Algebraic Equations of Multibody Dynamics". *Multibody System Dynamics,* **9**(2), pp. 121–142.

[18] Orlandea, N., Chace, M. A., and Calahan, D. A., 1977. "A sparsity-oriented approach to the dynamic analysis and design of mechanical systems – part I and part II". *Trans-*

actions of the ASME Journal of Engineering for Industry, pp. 773–784.

[19] Gear, C. W., Gupta, G., and Leimkuhler, B., 1985. "Automatic integration of the Euler-Lagrange equations with constraints". *J. Comp. Appl. Math.,* **12**, pp. 77–90.

[20] Fhrer, C., and Leimkuhler, B. J., 1991. "Numerical solution of differential-algebraic equations for constrained mechanical motion". *Numerische Mathematik,* **59**(1), pp. 55–69.

[21] Ascher, U. M., and Petzold, L. R., 1993. "Stability of computational methods for constrained dynamics systems". *SIAM Journal on Scientific Computing,* **14(1)**, pp. 95–120.

[22] Ascher, U. M., Chin, H., and Reich, S., 1994. "Stabilization of daes and invariant manifolds.". *Numerische Mathematik,* **67(2)**, pp. 131–149.

[23] Ascher, U. M., Chin, H., Petzold, L., and Reich, S., 1995. "Stabilization of constrained mechanical systems with daes and invariant manifolds.". *Mechanics of Structures and Machines,* **23(2)**, pp. 135–157.

[24] Lubich, C., Nowak, U., Pohle, U., and Engstler, C., 1995. "MEXX - numerical software for the integration of constrained mechanical multibody systems". *Mechanics of Structures and Machines,* **23**, pp. 473–495.

[25] Bauchau, O. A., Bottasso, C. L., and Trainelli, L., 2003. "Robust integration schemes for flexible multibody systems". *Computer Methods in Applied Mechanics and Engineering,* **192**, pp. 395 – 420.

[26] Hughes, T. J. R., 1987. *Finite Element Method - Linear Static and Dynamic Finite Element Analysis*. Prentice-Hall, Englewood Cliffs, New Jersey.

[27] Geradin, M., and Rixen, D., 1994. *Mechanical Vibrations: Theory and Application to Structural Dynamics*. Wiley, New York, NY.

[28] Hilber, H. M., Hughes, T. J. R., and Taylor, R. L., 1977. "Improved numerical dissipation for time integration algorithms in structural dynamics". *Earthquake Eng. and Struct. Dynamics,* **5**, pp. 283–292.

[29] Chung, J., and Hulbert, G. M., 1993. "A time integration algorithm for structural dynamics with improved numerical dissipation: the generalized-α method". *Transactions of ASME, Journal of Applied Mechanics,* **60**(2), pp. 371–375.

[30] Cardona, A., and Geradin, M., 1989. "Time integration of the equation of motion in mechanical analysis". *Computer and Structures,* **33**, pp. 801–820.

[31] Yen, J., Petzold, L., and Raha, S., 1998. "A time integration algorithm for flexible mechanism dynamics: The DAE α-method". *Computer Methods in Applied Mechanics and Engineering,* **158**, pp. 341–355.

[32] Negrut, D., Rampalli, R., Ottarsson, G., and Sajdak, A., 2007. "On the use of the HHT method in the context of index 3 Differential Algebraic Equations of Multibody Dynamics". *ASME Journal of Computational and Nonlinear Dynamics,* **2**.

[33] Bottasso, C. L., Bauchau, O. A., and Cardona, A., 2007. "Time-step-size-independent conditioning and sensitivity to perturbations in the numerical solution of index three differential algebraic equations". *SIAM Journal on Scientific Computing,* **3**, pp. 395–420.

[34] Newmark, N. M., 1959. "A method of computation for structural dynamics". *Journal of the Engineering Mechanics Division, ASCE*, pp. 67–94.

[35] Jay, L. O., and Negrut, D., 2006. "Extensions of the HHT-α method to differential-algebraic equations in mechanics". *Electronic Transactions on Numerical Analysis, accepted.*

[36] Lunk, C., and Simeon, B., 2006. "Solving constrained mechanical systems by the family of Newmark and α-methods". *ZAMM,* **86**, pp. 772–784.

[37] Jay, L. O., and Negrut, D., 2007. "A second order extension of the HHT-α method for constrained systems in mechanics". In Proceedings to the ECCOMAS thematic conference on Multibody Dynamics, ECCOMAS.

[38] Lötstedt, C., and Petzold, L., 46. "Numerical solution of nonlinear differential equations with algebraic constraints I: Convergence results for backward differentiation formulas". *Mathematics of Computation,* **174**, pp. 491–516.

[39] Brenan, K., and Engquist, B. E., 1988. "Backward differentiation approximations of nonlinear differential/algebraic systems". *Mathematics of Computation,* **51**(184), pp. 659–676.

[40] Schafer, N., Serban, R., and Negrut, D., 2007. "An investigation of new numerical methods for molecular dynamics simulation (DETC2007-35519)". *6th ASME International Conference on Multibody Systems, Nonlinear Dynamics and Control, Las Vegas, NV, ASME.*

[41] Shabana, A. A., and Yakoub, R. Y., 2001. "Three dimensional absolute nodal coordinate formulation for beam elements: Theory". *ASME Journal of Mechanical Design,* **123**, pp. 606–613.